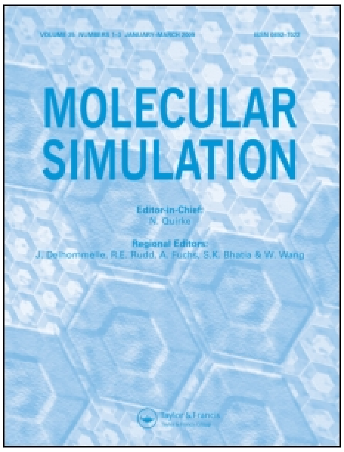

Molecular Simulation
Publication details, including instructions for authors and subscription information:
http://www.informaworld.com/smpp/title~content=t713644482

Observation of Liquid-to-Glass and Glass-to-Glass Transitions in L64/D²O Triblock Copolymer Micellar System

Sow-Hsin Chen[a]; Wei-Ren Chen[a]; Francesco Mallamace[b]
[a] Department of Nuclear Engineering, Massachusetts Institute of Technology, Cambridge, MA, USA [b] Department of Physics, University of Messina, Messina, Italy

To cite this Article Chen, Sow-Hsin , Chen, Wei-Ren and Mallamace, Francesco(2003) 'Observation of Liquid-to-Glass and Glass-to-Glass Transitions in L64/D²O Triblock Copolymer Micellar System', Molecular Simulation, 29: 10, 611 — 618

To link to this Article: DOI: 10.1080/0892702031000103149

URL: http://dx.doi.org/10.1080/0892702031000103149

Molecular Simulation, Vol. 29 (10–11), October–November 2003, pp. 611–618

Taylor & Francis
Taylor & Francis Group

Observation of Liquid-to-Glass and Glass-to-Glass Transitions in L64/D_2O Triblock Copolymer Micellar System

SOW-HSIN CHEN[a,*], WEI-REN CHEN[a] and FRANCESCO MALLAMACE[a,b]

[a]*Department of Nuclear Engineering, Massachusetts Institute of Technology, Cambridge, MA, 02139, USA;* [b]*Department of Physics, University of Messina, Messina, Italy*

(Received September 2002; In final form January 2003)

We report photon correlation spectroscopy (PCS), low shear viscosity and small angle neutron scattering (SANS) studies of a Pluronic L64 micellar system in aqueous solutions at high polymer concentrations (wt%), 35.0% < c < 54.4%, in a temperature range where a kinetic glass transition (KGT) has been observed. We analyze SANS intensity distributions in the liquid state assuming that the micelles are spherical and interact among themselves via an effective pair-potential consisting of a hard core plus a narrow attractive square-well, the depth of which is temperature dependent. Comparison of the potential parameters so obtained with the phase diagram predicted recently by mode coupling theory (MCT) allows us to verify the existence of the so-called "liquid to attractive glass" KGT line. We then use scaling plots of SANS intensity distributions to show the existence of another branch of the KGT line where transitions from a repulsive glass to an attractive glass occur. In particular, we show an evidence of the existence of the so-called A_3 singularity end point where two glasses become identical in local structure [Sow-Hsin Chen, Wei-Ren Chen, Francesco Mallamace, "The glass–glass transition and its end point in a co-polymer micellar system", to be published].

Keywords: Photon correlation spectroscopy; Low shear viscosity; SANS; Pluronic L64 micellar system

INTRODUCTION

In a recent series of papers [2,–4], it has been theoretically predicted that in colloidal systems with sufficiently short-range effective inter-particle attractive interaction, one has a possibility of observing two types of structural arrest transitions (SAT) or kinetic glass transitions (KGT). The KGT can be the result of a "cage effect" originating from the excluded volume effect of the particles at high volume fractions and at high temperatures or the result of a particle bonding to its nearest neighbors at low k_BT and at an extended range of volume fractions. If the interaction is modeled by a square-well potential, the crucial control parameters of the phase behavior are: the volume fraction, $\phi = \pi\rho d^3/6$, the effective temperature, $T^* = k_BT/u$, and the fractional well-width parameter, $\varepsilon = \Delta/d$, where ρ is the number density of the spheres, d its hard core diameter, Δ its attractive well-width, and $-u$ its well-depth. One particularly interesting feature in this novel state of matter is the occurrence of two distinct amorphous glassy states called, respectively, the "repulsive glass" and the "attractive glass", as the result of the two distinct mechanisms for the SAT mentioned earlier.

Figure 1 gives the experimental phase diagram of the L64/D_2O micellar system plotted in the (T,c) plane. It contains our previous discoveries of the cloud point line (solid line) and its associated critical point (black diamond spot) [5]; critical micelle concentration—critical micelle temperature line (dash-dotted line) [6]; percolation line (empty circles) [6]; equilibrium liquid-to-crystal phase boundary (dotted line) [7]; equilibrium crystal-to-crystal phase boundary (dash line) [7] and the KGT lines verified by three different experimental methods (symbols) [8,9].

Figure 2a gives the experimental phase diagram re-plotted in the (T,ϕ) plane [9]. It contains

---

*Corresponding author.

ISSN 0892-7022 print/ISSN 1029-0435 online
DOI: 10.1080/0892702031000103149

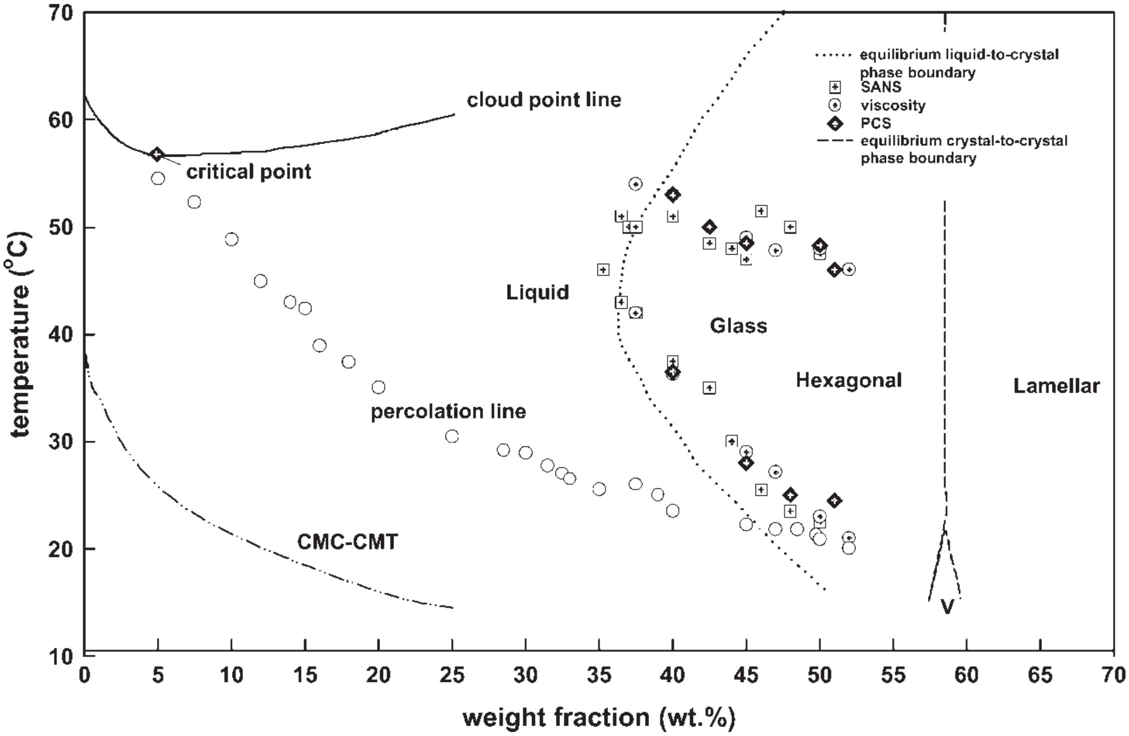

FIGURE 1 The phase diagram of Pluronic L64/D_2O solution. The phase diagram contains the CMC-CMT line (dash-dotted line), cloud point line (solid line), percolation line (empty circles), the equilibrium liquid-to-crystal phase boundary (dotted line), the equilibrium crystal-to-crystal phase boundary (dash line) and the re-entrant kinetic glass transition (KGT) lines (symbols) which are determined by PCS, SANS and low shear viscosity measurements, respectively.

the equilibrium liquid-to-crystal phase boundary (solid line), the KGT line (dash line) and the phase points where the experimental data are analyzed. The calculated KGT lines, for the case of $\varepsilon = 0.03$ [10], are shown in Fig. 2b in the (T,ϕ) plane. As one can see, at volume fractions less than 0.5365, one has liquid-to-attractive glass transitions if one lowers T^*, and at volume fractions greater than this value, one has a possibility of observing a repulsive glass-to-attractive glass transitions by going from high T^* to low T^*. With photon correlation spectroscopy (PCS) and small angle neutron scattering (SANS) measurements, we succeeded in detecting both transitions in L64/D_2O micellar system at high volume fractions as we shall describe later [9].

MICELLAR SYSTEM

Polyethylene oxide (PEO) and polypropylene oxide (PPO) containing block copolymers belong to a class of polymers that self-associate spontaneously in aqueous solution. The self-association is characterized by sensitivity to temperature [11]. The most interesting feature of Pluronic copolymers is the resultant formation of rich phase behavior of the solutions upon self-assembly [12]. In particular, many triblock copolymers composed of two symmetric end-block PEOs and a middle-block PPO have been synthesized and used as polymeric surfactants. These triblock copolymers we studied are commercially available under a trade name Pluronic from BASF [13]. Pluronic polymer surfactants find widespread industrial applications as detergents, wetting, foaming/defoaming, emulsification, lubrication and solublization agents [13].

The L64, with a chemical composition of $(PEO)_{13}$ $(PPO)_{30}(PEO)_{13}$, is a member of this symmetric triblock copolymers family with PEO–PPO is 40: 60 (by weight). At low temperatures, both PEO and PPO are hydrophilic and readily dissolve in water, forming unimers. However, as temperature rises above 20°C, they rapidly loose their hydrophilicity in different degrees, PPO segments becoming less hydrophilic faster than PEO segments. The copolymers thus acquire surfactant property. If the temperature is above a critical micelle temperature which is a function of concentration (called C.M.T and C.M.C., respectively), they will self-assemble into spherical micelles each with PPO segments packed into a compact core and PEO segments forming a corona region around it carrying substantial amount of hydration water [14,15]. The short-range attraction arises from small overlapping of PEO chains of the corona regions when micelles touch each other, expelling some solvent molecules from the corona regions. The depth of the attractive well increases with temperature because water

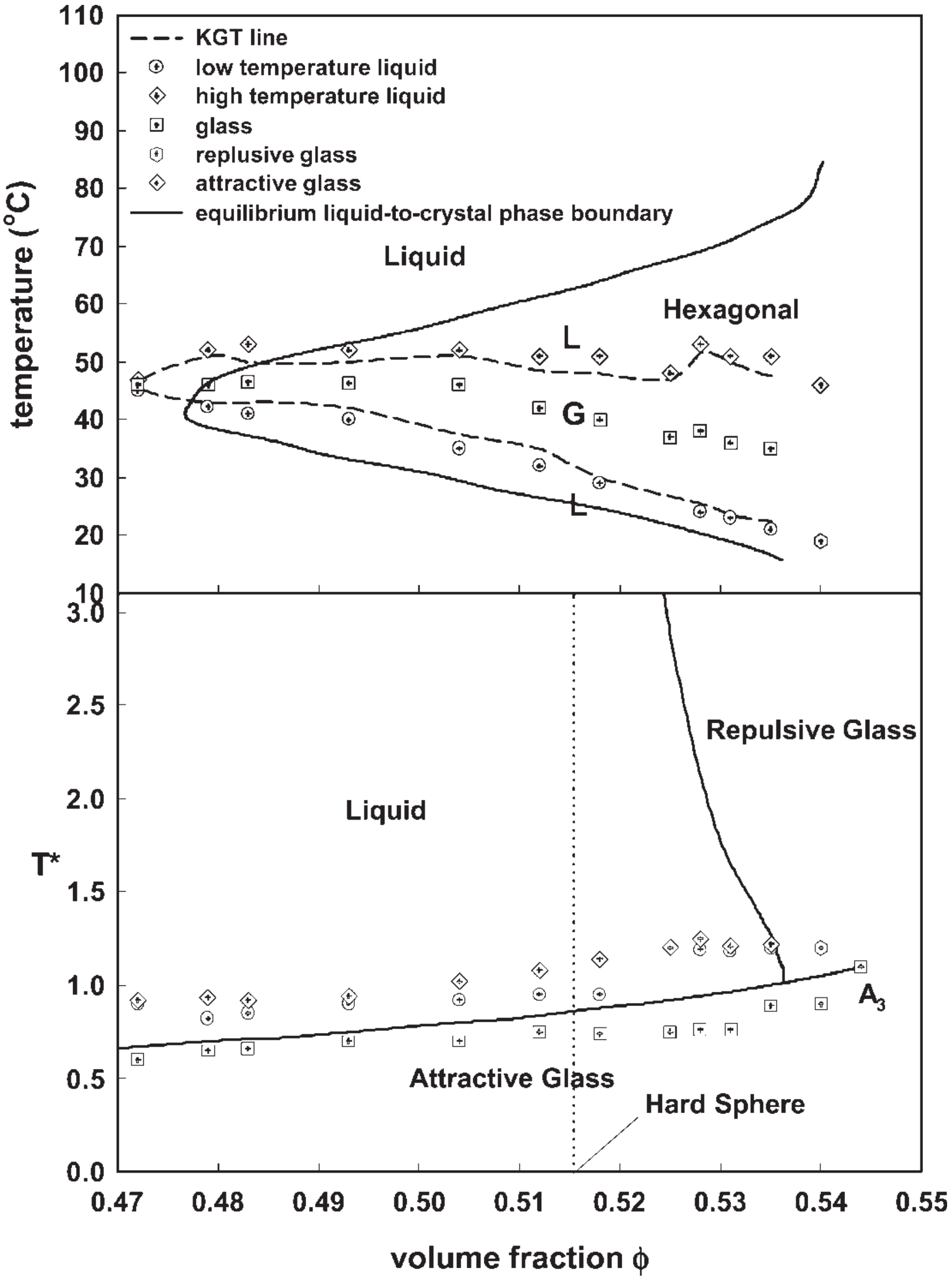

FIGURE 2 Comparison of the phase diagram (in T−ϕ plane) of L64/D$_2$O micellar solution with that of the theoretical phase diagram (in T^*−ϕ plane) determined by mode coupling theory (MCT) for a colloidal system with a short range attraction ($\varepsilon = 0.03$). In the phase diagram given on the top panel, the solid line is the equilibrium liquid-to-crystal transition line, dash line the re-entrant KGT line and symbols the phase points where the experimental data are analyzed. The lower panel gives the theoretical phase diagram of a colloidal system interacting via a short-range attractive square well potential predicted by MCT. The phase points shown in the upper panel are then mapped into the corresponding symbols in the lower panel using the results of SANS data analyses. The result of the mapping is seen to confirm the existence of the attractive branch in the predicted KGT boundary and the repulsive glass-to-attractive glass transition section.

becomes increasingly poor solvent as temperature rises.

Gelation of Pluronic solutions occurs at high polymer concentrations. This is traditionally interpreted as formation of an ordered liquid crystalline phase, distinct from the disordered micellar phase. For the 40% PEO Pluronic family, such as L64, concentration of the sol−gel transition is only weakly dependent on temperature. In Fig. 1, the gelation boundary is marked by a dash line with the lowest concentration occurring at $c = 35\%$ and $T = 40$°C. These gelation concentrations set the upper limit for the concentration range of the disordered micellar phase. It is in this gelation concentration range of L64/D$_2$O solutions that we found the KGT phenomena. Experimentally, we found that if we enter this region of gel phase from the low temperature side, the system will take a long time (of the order of weeks) to reach its equilibrium crystalline state without an external perturbation, such as applying a shear stress to the sample.

EXPERIMENTAL RESULTS

SANS Data Analysis [9]

We observed that at high enough polymer concentration, a SANS intensity distribution from the L64/D_2O micellar system generally consists of a single, sharp interaction peak. A series of SANS intensity distributions taken from the micellar solutions with different polymer concentrations and temperatures have been examined to see whether there is a significant change of the line shape at the ergodic-to-non-ergodic-to-ergodic transition temperatures observed by PCS experiment which we shall show later in Fig. 4. Since there is a single peak in the observed SANS intensity distribution, we can assume that the system is characterized by a single length scale $\Lambda = 1/k_{\max}$ where $k_{\max}$ is the peak position of the intensity distribution. Λ in this case, can be taken as the mean particle separation in the disorder state. It is well known that the absolute intensity in a two-phase system (the micelles and the solvent) is given by a 3D Fourier transform of the Debye correlation function $\Gamma(r)$ and the Debye correlation function in this case must be of the form $\Gamma(r/\Lambda)$. Therefore

$$I(k) = \langle \varsigma^2 \rangle \int_0^\infty \mathrm{d}r\, 4\pi r^2 j_0(kr)\Gamma\left(\frac{r}{\Lambda}\right) \qquad (1)$$

where $\langle \varsigma^2 \rangle$ is the so-called "invariant".

Now, make a transformation of variables, $x = (r/\Lambda) = k_{\max} r$, $y = \frac{k}{k_{\max}}$.

Then

$$\frac{k_{\max}^3 I(k)}{\langle \varsigma^2 \rangle} = \int_0^\infty \mathrm{d}x 4\pi x^2 j_0(xy)\Gamma(x). \qquad (2)$$

Thus it can be seen that the scaled intensity $(k_{\max}^3 I(k))/\langle \varsigma^2 \rangle)$ is a unique function of scaled variable $y = k/k_{\max}$. Therefore, if we plot the scaled intensity distributions at different temperatures as a function of y, they will all collapse into one single master curve, if the degree of disorder of the system remains the same.

Figure 3 shows scaling plots of SANS intensity distributions at four volume fractions (ϕ determined by fitting of the SANS data) and different temperatures, spanning the regions of the phase diagram where the liquid-to-liquid, liquid-to-glass, glass-to-glass and two identical glasses (A_3 point) are located. This kind of scaling plot is very useful for visualization of the degree of order of the system characterized by a unique length scale (the average inter-particle distance). We thus demonstrated for the first time that SANS measurements can be a powerful tool for studying the SAT in dense colloidal solutions predicted by mode coupling theory (MCT) formulated originally for supercooled simple liquids [16].

We also analyzed the SANS intensity distributions directly using the liquid theory. The absolute intensity (in unit of cm^{-1}) of neutron scattering from a system of mono-dispersed micelles can be express by the following formula [14]:

$$I(k) = cN\left(\sum_i b_i - \rho_{\mathrm{w}} v_{\mathrm{p}}\right)^2 \bar{P}(k)S(k) \qquad (3)$$

where c is the concentration of polymer (number of polymers/cm^3), N the aggregation number of polymers in a micelle, $\sum_i b_i$ sum of coherent scattering lengths of atoms comprising a polymer molecule, ρ_{w} the scattering length density of D_2O, v_{p} the molecular volume of the polymer, $\bar{P}(k)$ the normalized intra-particle structure factor (of the micelle) and $S(k)$ the inter-particle structure factor (between micelles). $\bar{P}(k)$ is computed by a modified cap-and-gown model described in [9]. $S(k)$ can be obtained by solving the Ornstein-Zernike (OZ) equation in Percus-Yevick (PY) approximation for the square well potential to the first order in a series of small ϵ expansion [17]. To fit SANS data, the Eq. (3) is convoluted with the Gaussian-like resolution functions supplied by Center of Neutron Research in NIST and Intense Pulse Neutron Source in ANL, respectively. From the fitting of a SANS intensity distribution, we obtained the four parameters: the aggregation number N, the volume fraction ϕ, the fractional well width parameter ε and the effective temperature T*. The normalized intra-particle structure factor $\bar{P}(k)$ is the function of N only. The inter-micellar structure factor $S(k)$ is the function of all the four parameters. From fitting of a SANS intensity distribution taken at a state (c,T), we can then obtain the corresponding set of parameters (ϕ, T*). Thus we can map a phase point from the experimental c–T plane onto a corresponding point in the ϕ–T* plane on which the theoretical phase diagram is constructed. The result of such a mapping is shown by symbols in Fig. 2b. As one can see, this mapping confirms the existence of the attractive branch of the KGT line and the repulsive glass to attractive glass transition section of it as well.

PCS Data

Figure 4 shows three sets of normalized photon correlation functions (coherent intermediate scattering functions, ISF) measured at $k \approx 0.002\text{Å}^{-1}$and at three different volume fractions, as a function of

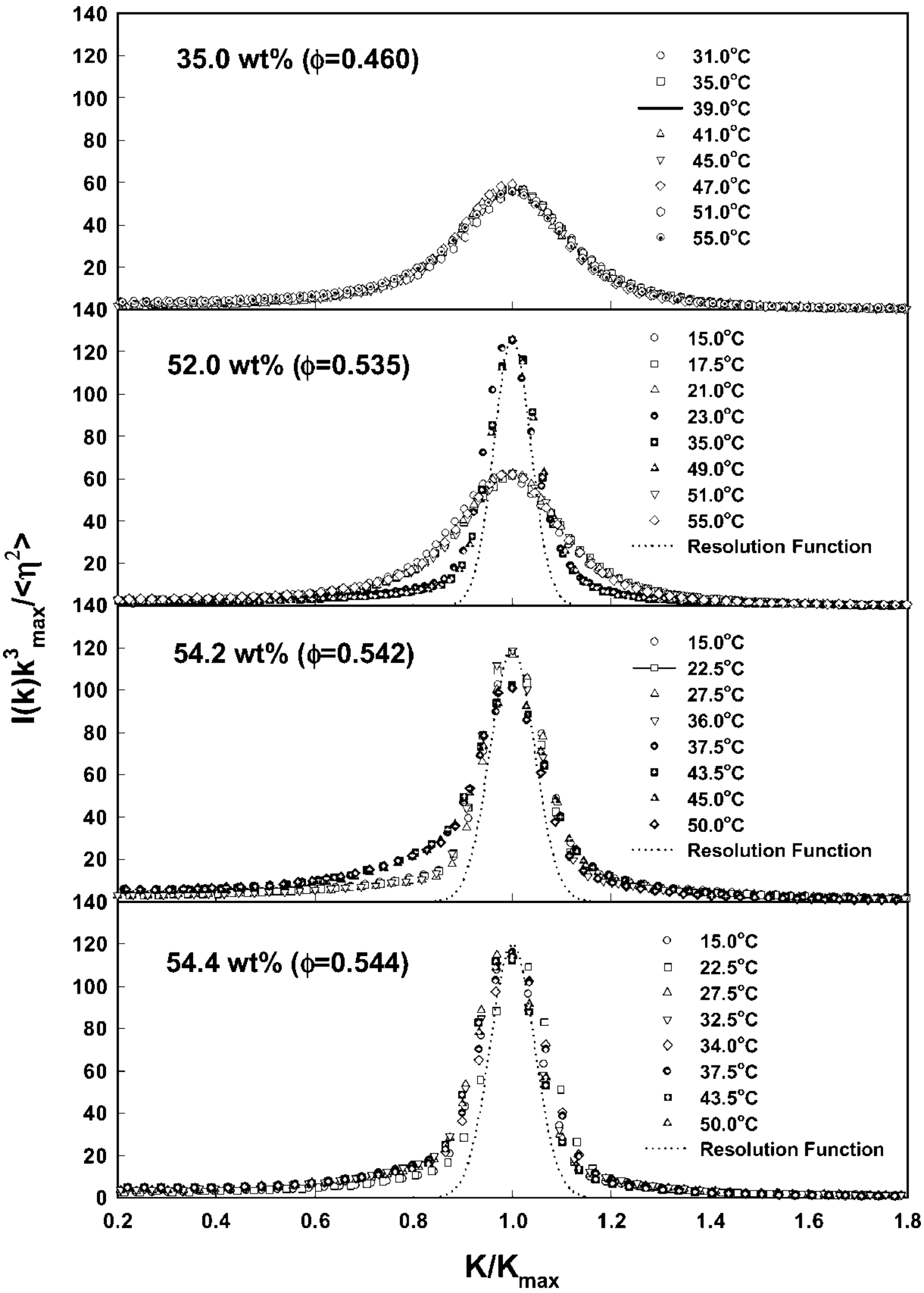

FIGURE 3 Typical examples of the scaling plots of SANS intensity distributions at four different concentrations as a function of temperature. The first panel gives SANS intensity distributions of the micellar solution at $\phi = 0.460$, and at different temperatures. It can be seen that all the scaled intensities are characterized by a unique length scale and collapse into a single master curve, independent of temperatures. The scaling plots of $\phi = 0.535$ micellar solutions at different temperatures are given in the second panel. It is seen clearly that the system is still characterized by a temperature dependent length scale, but there are two distinct disorder (width of the peak) depending on temperature. While the narrower peak is resolution limited, the broader peak is similar to the one observed in the first panel. If we identify the broader peak to represent the liquid state, then the narrower peak should represent the glassy state. It is seen from this plot that the system shows a re-entrant liquid-to-glass-to-liquid transition. The third panel represents the scaling plots of a micellar solution at $\phi = 0.542$ at different temperatures. It is seen that the system is again characterized by a temperature dependent length scale. While the narrower peak is resolution limited, the slightly broader peak is also nearly resolution limited. It can be interpreted as showing a glass-to-glass transition (transition between two amorphous solid states with different degrees of disorder). The last panel shows the scaling plots of the micellar solution at $\phi = 0.544$, which is predicted as the A_3 point, at temperatures range from 15 to 50°C. It can be seen that two different types of glasses indeed become identical at this concentration.

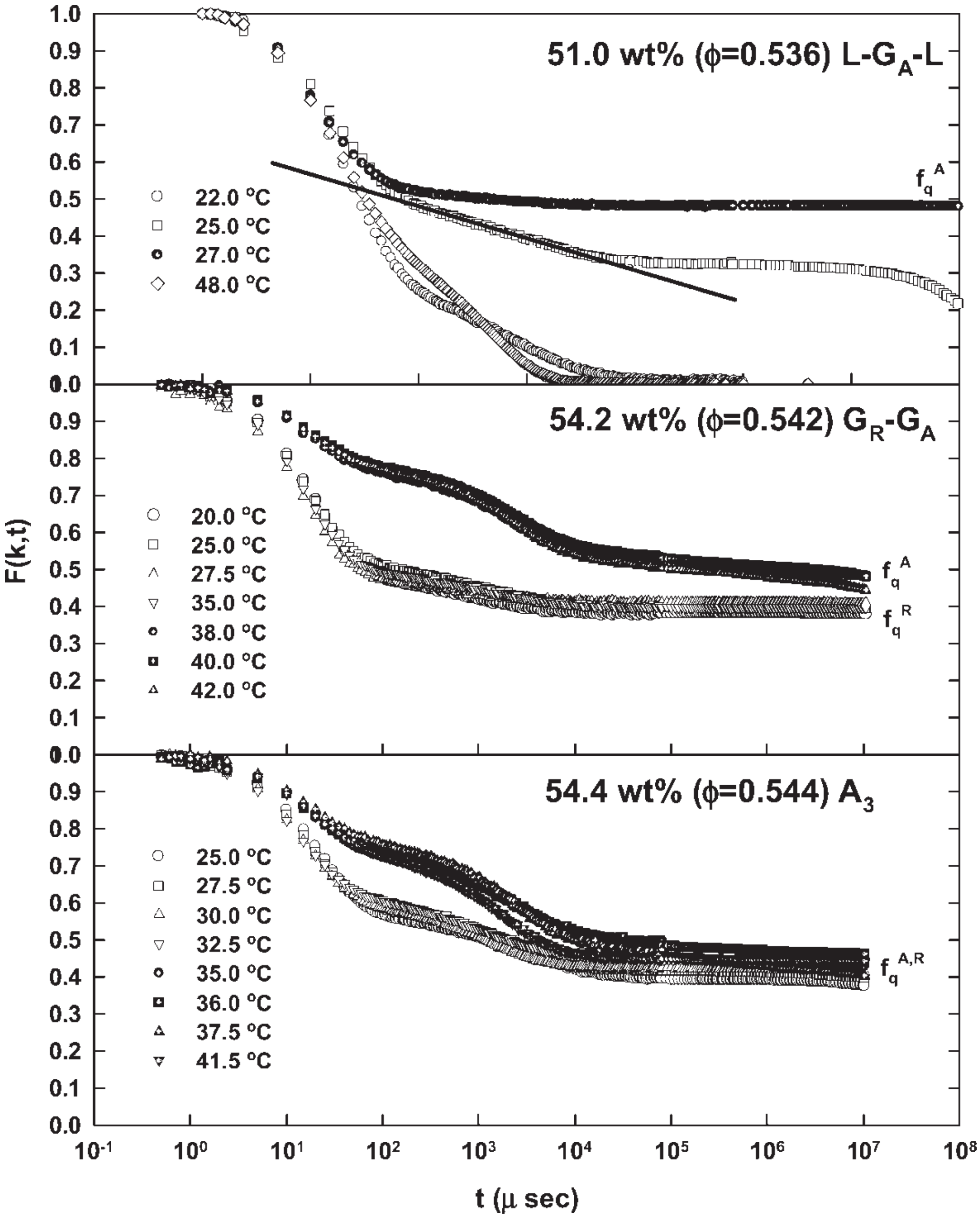

FIGURE 4 Three examples of the intermediate scattering functions, $F(k,t)$, as measured by photon correlation spectroscopy (PCS), at different concentrations, as a function of temperature. The top panel shows the liquid-to-attractive glass-to-liquid (i.e. ergodic-to-non-ergodic-to-ergodic) transition. We also highlight the occurrence of a region of the logarithmic time dependence preceding the plateau region for the system in the ergodic state just before the transition. The evidence of the attractive glass-to-repulsive glass transition can be seen in the middle panel. By comparing the long time limit of the ISF's with the predictions of MCT, the two different types of the glasses can be identified by the respective Debye-Waller factors $f_q^A \approx 0.5$ and $f_q^R \approx 0.4$. The bottom panel gives the intermediate scattering functions at volume fraction of 0.544, which is the A_3 end point predicted by MCT. Our ISF's show that the Debye-Waller factors of the two glasses become identical, confirming the prediction of the MCT.

temperature. For the lowest volume fraction where the liquid to attractive glass transition is predicted, one can see that in the liquid state, the long-time limit of the ISF, f_q, is zero, while in the attractive glass state $f_q^{\mathrm{A}} \approx 0.5$, which is the Debye-Waller factor of the attractive glass state [9]. The SAT is thus characterized by a discontinuous change of f_q, called a bifurcation transition [18]. At volume fraction of 0.542, we observe the repulsive glass ($f_q^{\mathrm{R}} \approx 0.4$) to attractive glass transition ($f_q^{\mathrm{A}} \approx 0.5$). At volume fraction of 0.544, which is called the A_3 singularity point, where according to the theory, the two glasses become identical [3]. Our measured ISF's indeed verify that it is so, showing an identical value of $f_q^{\mathrm{A,R}} \approx 0.45$ in the two glass states. This observation of the A_3 singularity is made by us for the first time [1].

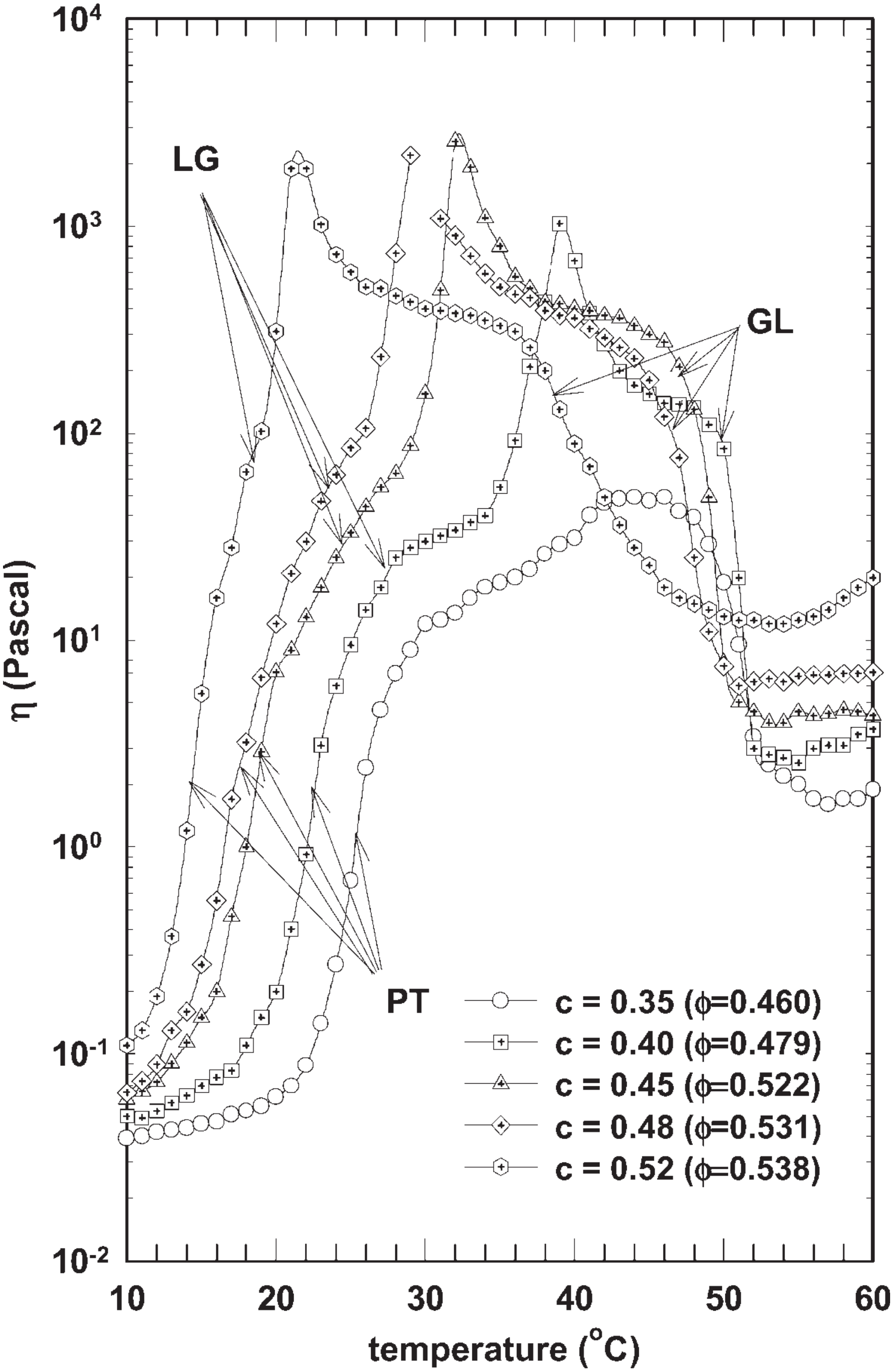

FIGURE 5 The low shear viscosity at five different concentrations, where only glass-to-liquid-to-glass transition is possible, as a function of temperature. Starting from low temperatures, the shear viscosity increases steeply, first going through a percolation transition (PT), then a liquid-to-glass transition (LG) and finally a glass-to-liquid transition (GL). Note that, for the case of $c = 0.35$, there is only the PT.

Viscosity Data [9]

The low shear viscosity at five different concentrations measured as a function of the temperature is shown in Fig. 5. The viscosities at all concentrations are characterized by an initial increase, starting from a viscosity value typical of a liquid ($\eta \approx 10^{-2}$ Pa), followed by a flatten-off at the highest temperatures ($\eta \approx 10^{3}$ Pa). For the concentration, $c = 35\%$, the viscosity shows only a single step increase that covers three orders of magnitude. For the remaining concentrations, there is an additional step increase located in a different temperature range. Thus for concentrations $c > 35\%$, the overall viscosity increase is about five orders of magnitude. The first step viscosity increase in L64/D_2O micellar system is due to the percolation process that is characteristic of a colloid with a short-range attractive interaction [6]. Comparing with SANS and PCS measurement, we concluded that the sharp reduction in viscosity and its eventual flatten-off at high temperatures (with final viscosity value of the order of a few Pascal) can be related to the re-entry of the system into the liquid state.

CONCLUSIONS

Recent MCT calculations show that, for a colloidal system with short-range attractive inter-particle interactions, the features of the phase diagram, like the one presented in Fig. 2b, is insensitive to the detail shape of the attractive part of the interaction [4,19]. In this paper, our results confirm the phase boundaries of predicted KGT through three different experimental approaches: we use SANS results and their analyses to verify the existence of the liquid-to-attractive glass and repulsive glass-to-attractive glass branch of KGT line; we use combination of scaling plots of the SANS data and PCS results to give a conclusive evidence of the existence of the A_3 singularity where the local structure and the long time dynamical behavior of the two glasses become identical.

Acknowledgements

The research at MIT is supported by a grant from Materials Science Division of US DOE. The research in Messina is supported by INFM-PRA98 and MURST-PRIN2000. We are indebted to Dr Emiliano Fratini for purifying L64 samples. We also wish to acknowledge stimulating discussions with professor Piero Tartaglia and professor Kenneth A. Dawson. Finally we are grateful to Dr Charles Glinka and Dr Derek Ho of CNR (NIST) and Dr Papanan Thiyagarajan of IPNS (ANL) for the beam time of NG7 and SAND spectrometers respectively and for their technical assistances.

References

[1] Sow-Hsin Chen, Wei-Ren Chen and Francesco Mallamace, "The glass–glass transition and its end point in a co-polymer micellar system", to be published.

[2] Fabbian, L., Götze, W., Sciortino, F., Tartaglia, P. and Thiery, F. (1999) "Ideal glass–glass transition and logarithmic decay of correlations in a simple system", *Phys. Rev. E* **59**, R1347.

[3] Dawson, K.A., Foffi, G., Fuchs, M., Götze, W., Sciortino, F., Sperl, M., Tartaglia, P., Voigtmann, Th. and Zaccarelli, E. (2001) "Higher-order glass-transition singularities in colloidal systems with attractive interactions", *Phys. Rev. E* **63**, 011401.

[4] Dawson, K.A. (2002) "The glass paradigm for colloidal glasses, gels, and other arrested states driven by attractive interactions", *Curr. Opin. Coll. Interface Sci.* **7**, 218–227.

[5] Liao, C., Choi, S.M., Mallamace, F. and Chen, S.H. (2000) "SANS study of the structure and interaction of L64 triblock copolymer micellar solution in the critical region", *J. Appl. Crystallogr.* **33**, 677.

[6] Lobry, L., Micali, N., Mallamace, F., Liao, C. and Chen, S.H. (1999) "Interaction and percolation in the L64 triblock copolymer micellar system", *Phys. Rev. E* **60**, 7076.

[7] Zhang, K.Z., Lindman, B. and Coppola, L. (1995) "Melting of block-copolymer self-assemblies induced by a hydrophilic surfactant", *Langmuir* **11**, 538.

[8] Mallamace, F., Gambadauro, P., Micali, N., Tartaglia, P., Liao, C. and Chen, S.H. (2000) "Kinetic glass transition in a micellar system with short-range attractive interaction", *Phys. Rev. Lett.* **84**, 5431.

[9] Chen, W.R., Chen, S.H. and Mallamace, F. (2002) "Small-angle neutron scattering study of the temperature-dependent attractive interaction in dense L64 copolymer micellar solutions and its relation to kinetic glass transition", *Phys. Rev. E* **66**, 021403.

[10] Zaccarelli, E., Foffi, G., Dawson, K.A., Sciortino, F. and Tartaglia, P. (2001) "Mechanical properties of a model of attractive colloidal solutions", *Phys. Rev. E* **63**, 031501.

[11] Lindman, B., Carlsson, A., Karlstrom, G. and Malmsten, M. (1990) "Nonionic polymers and surfactants—some anomalies in temperature dependence and in interactions with ionic surfactants", *Adv. Coll. Interface Sci.* **32**, 183.

[12] Alexandridis, P. and Hatton, T.A. (1995) "Poly(Ethylene Oxide)–Poly(Propylene Oxide)–Poly(Ethylene Oxide) block-copolymer surfactants in aqueous-solutions and at interfaces—thermodynamics, structure, dynamics, and modeling", *Coll. Surf.* **96**, 1.

[13] Pluronic and Technical Brochure for Tetronic Surfactants. BASF Corp., Parsipanny, NJ (1989).

[14] Liu, Y.C., Chen, S.H. and Huang, J.S. (1998) "Small-angle neutron scattering analysis of the structure and interaction of triblock copolymer micelles in aqueous solution", *Macromolecules* **31**, 2236.

[15] Chen, S.H., Liao, C., Fratini, E., Baglioni, P. and Mallamace, F. (2001) "Interaction, critical, percolation and kinetic glass transitions in pluronic L-64 micellar solutions", *Coll. Surf., A* **95**, 183.

[16] Götze, W. and Sjögren, L. (1992) "Relaxation processes in supercooled liquids", *Rep. Prog. Phys.* **55**, 241.

[17] Liu, Y.C., Chen, S.H. and Huang, J.S. (1996) "Relationship between the microstructure and rheology of micellar solutions formed by triblock copolymer surfactant", *Phys. Rev. E* **54**, 1698.

[18] Götze, W. (1991) "Aspects of structural glass transitions in *Liquids*", In: Hansen, J.P., Levesque, D. and Zinn-Justin, J., eds, *Liquid, Freezing and Glass Transition* (North-Holland, Amsterdam).

[19] Foffi, G., McCullagh, G.D., Lawlor, A., Zaccarelli, E., Dawson, K.A., Sciortino, F., Tartaglia, P., Pini, D. and Stell, G. (2002) "Phase equilibria and glass transition in colloidal systems with short-ranged attractive interactions: application to protein crystallization", *Phys. Rev. E* **65**, 031407.